eLIFE elifesciences.org

RESEARCH ARTICLE

Figures and figure supplements

A gut bacterial amyloid promotes α-synuclein aggregation and motor impairment in mice

Timothy R Sampson *et al*

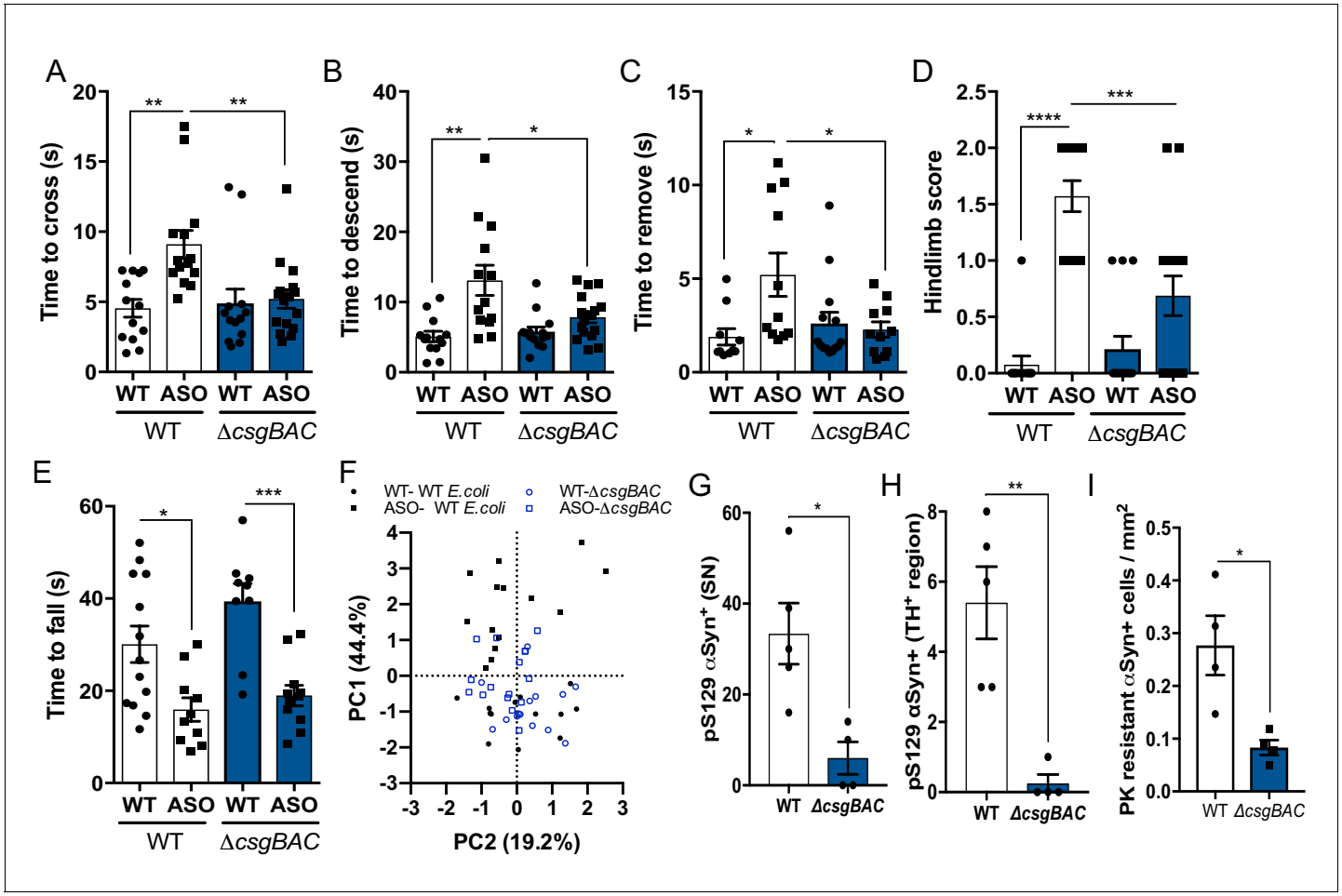

Figure 1. Mono-colonization with curli-producing gut bacteria enhances αSyn pathophysiology germ-free wild-type BDF1 (WT) and Thy1-αSyn (ASO) mice were mono-colonized with wild-type *E. coli* MC4100 (WT) or an isogenic curli-deficient strain (Δ*csgBAC*) at 5–6 weeks of age. Motor function was assessed at 12–13 weeks of age by quantifying (**A**), beam traversal time, (**B**), pole descent time, (**C**), nasal adhesive removal time, (**D**), hindlimb clasping score, (**E**), wirehang time. (**F**), Principal component analysis of compiled motor scores from tests in (**A–E**). Quantification of (**G, H**) pS129αSyn and (**I**) proteinase K–resistant αSyn by immunofluorescence microscopy in the substantia nigra and midbrain. n = 13–16 (**A–F**), n = 4.5 (**G–I**). Points represent individuals, bars represent the mean and standard error. Data analyzed by one-way ANOVA with Tukey post-hoc test (**A–E**), and two-tailed *t*-test for (**G–I**). *p≤0.05; **p≤0.01; ***p≤0.001; ****p≤0.0001. Motor data are compiled from three independent cohorts.

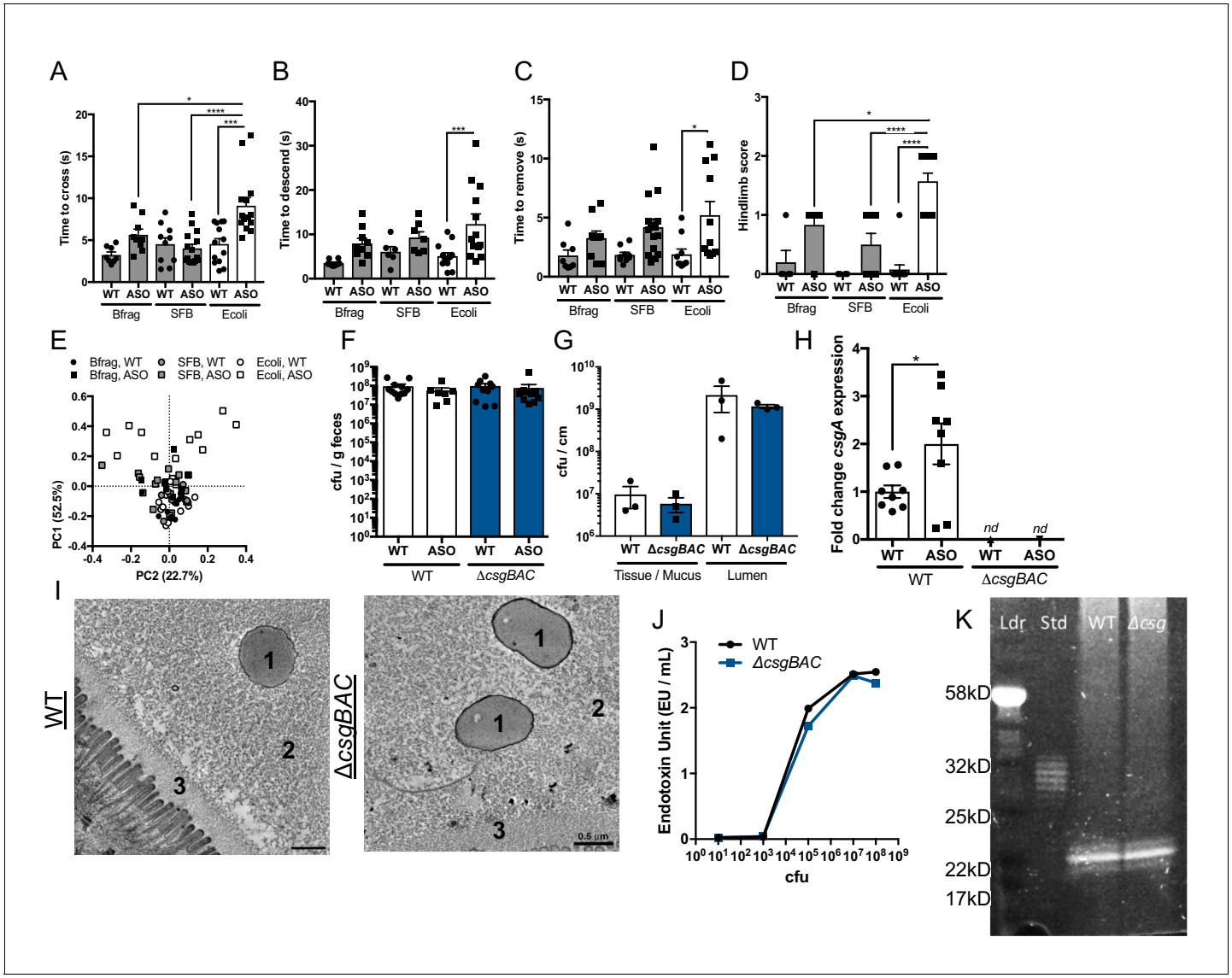

Figure 1—figure supplement 1. *E. coli* alters motor deficits, and CsgA does not influence colonization, inflammatory capacity, or dopamine production Germ-free (GF) wild-type (WT) or Thy1- αSyn (ASO) mice were mono-colonized with either *Bacteroides fragilis* (Bfrag), segmented filamentous bacteria (SFB), or *Escherichia coli* (Ecoli). Motor function assessed by (**A**) beam crossing time, (**B**) pole descent time, (**C**) adhesive removal time, or **D**) hindlimb reflex score.(**E**,) PCA analysis of scores in (**A–D**). (**F–N**) GF WT and ASO mice were mono-colonized with curli-sufficient *E. coli* (WT) or curli-deficient *E. coli* (Δ*csgBAC*). (**F**) Fecal bacterial burden determined by plate culture. (**G**) Bacterial burden of tissue/mucus fractions and luminal fractions of proximal colon. (**H**) *csgA* expression within fecal contents determined by qRT-PCR. (**I**) Representative TEM of bacterial localization in the proximal colon. 1- Bacteria, 2-mucus layer, 3-glycocalyx. (**J**) Quantification of endotoxin as determined by LAL assay. (**K**) Pro-Q Emerald stain (LPS) of SDS-PAGE separated cell lysates, Ldr- ladder, Std- LPS standard, WT- wild-type, Δcsg- Δ*csgBAC*. n = 7–14 (**A–E**); n = 7–9 (**F, H**); n = 3 (**G**). Points represent individuals, bars represent the mean and standard error. Data analyzed by one-way ANOVA with Tukey post-hoc test (**A–D**). *p≤0.05; **p≤0.01; ***p≤0.001; ****p≤0.0001. In (**A–D**), data are compiled from two independent cohorts for *B. fragilis* and SFB, compared to *E. coli* mono-colonized cohorts used in ***Figure 1***.

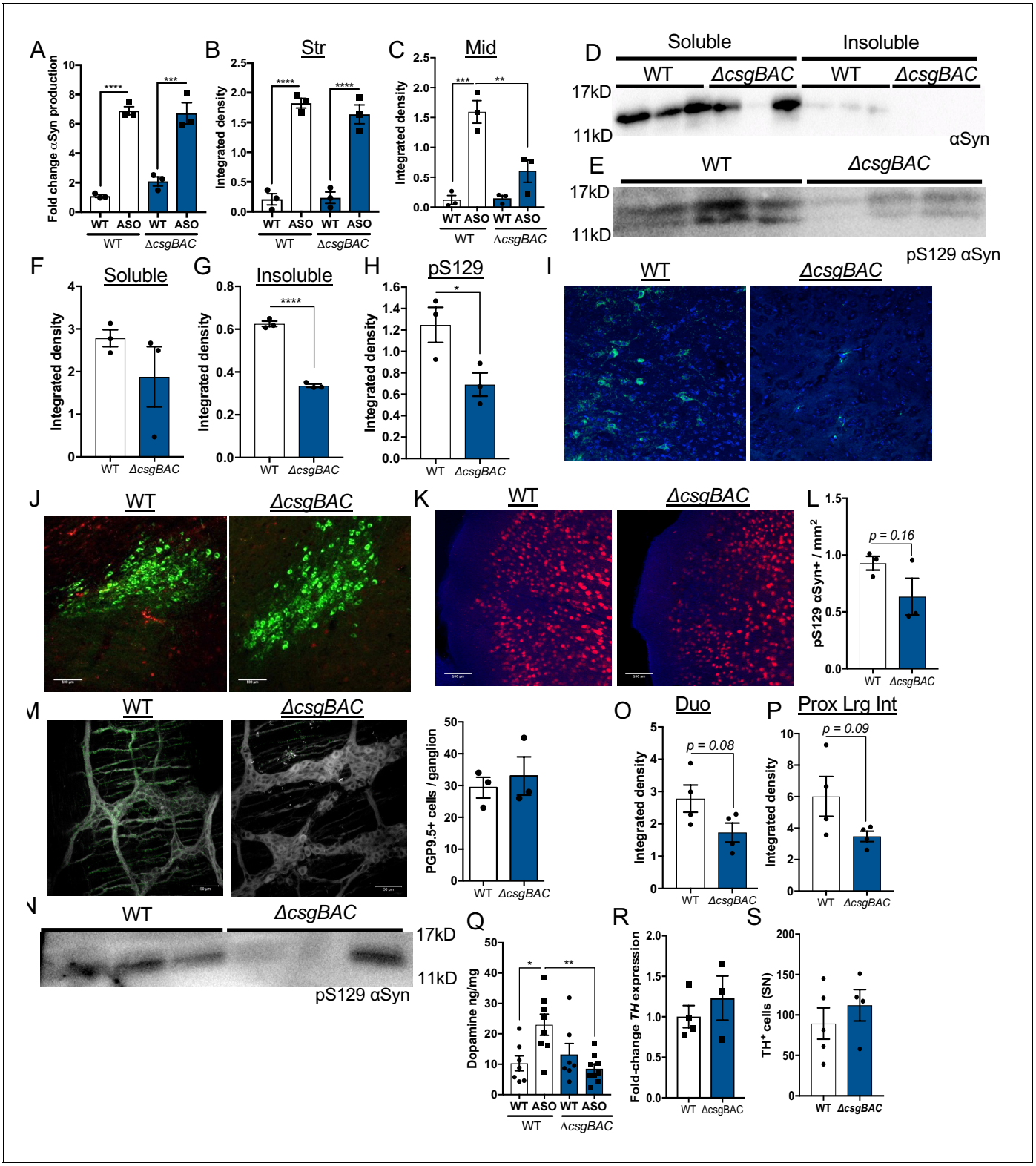

Figure 1—figure supplement 2. Mono-colonization with curli-sufficient bacteria induce increased αSyn-dependent pathology Germ-free (GF) wild-type (WT) or Thy1-αSyn (ASO) animals were mono-colonized with curli-sufficient *E. coli* (WT) or curli-deficient *E. coli* (Δ*csgBAC*). (**A**) Total αSyn in whole brain lysates quantified by ELISA. Quantification of insoluble αSyn fibrils in the (**B**) striatum and (**C**) midbrain by dot blot assay. Midbrain homogenates of ASO animals were (**D**) fractionated with Triton X-100 and SDS-PAGE, and subsequently probed for alpha-synuclein (αSyn) via western blot, or (**E**) left unfractionated and assessed by western blot for phospho-Serine129 αSyn (pS129). (**F–H**) Quantification of western blots by integrated density.

Figure 1—figure supplement 2 continued on next page

Figure 1—figure supplement 2 continued

Representative images from of mono-colonized ASO mice of the (**I**) midbrain stained for proteinase K-resistant αSyn (green), (**J**) substantia nigra stained for tyrosine hydroxylase (TH, green) and pS129 (red), and (**K**) frontal cortex stained for pS129 (red) and quantified in (**L**). (**M**) Representative images of the myenteric plexus within proximal large intestine of mono-colonized ASO animals stained for PGP9.5 (white) and pS129αSyn (green,), and counts of PGP9.5+ cells bodies per ganglia. (**N**) Proximal large intestine homogenates of mono-colonized ASO animals were assessed by SDS-PAGE and analyzed by western blot for pS129αSyn. Quantification of insoluble αSyn fibrils in the (**O**) duodenum and (**P**) proximal large intestine by dot blot assay. (**Q**) Total striatal dopamine quantified by ELISA. (**R**) *TH* expression in the midbrain by qPCR. (**S**) Quantification of TH+ cells in representative sections of the SN. n = 3 (**A–H, L**), n = 4 (**O, P**), n = 7–9 (**Q**), n = 3–4 (**R**), n = 4–5 (**S**). Full-length immunoblots available in associated Source Data file. Points represent individuals, bars represent the mean and standard error. Data analyzed by one-way ANOVA with Tukey post-hoc test for **A-C, Q**, or two-tailed *t*-test for **F-H, L, O, P, R, S**. *p≤0.05; **p≤0.01; ***p≤0.001; ****p≤0.0001. Scale bars = 100 μm.

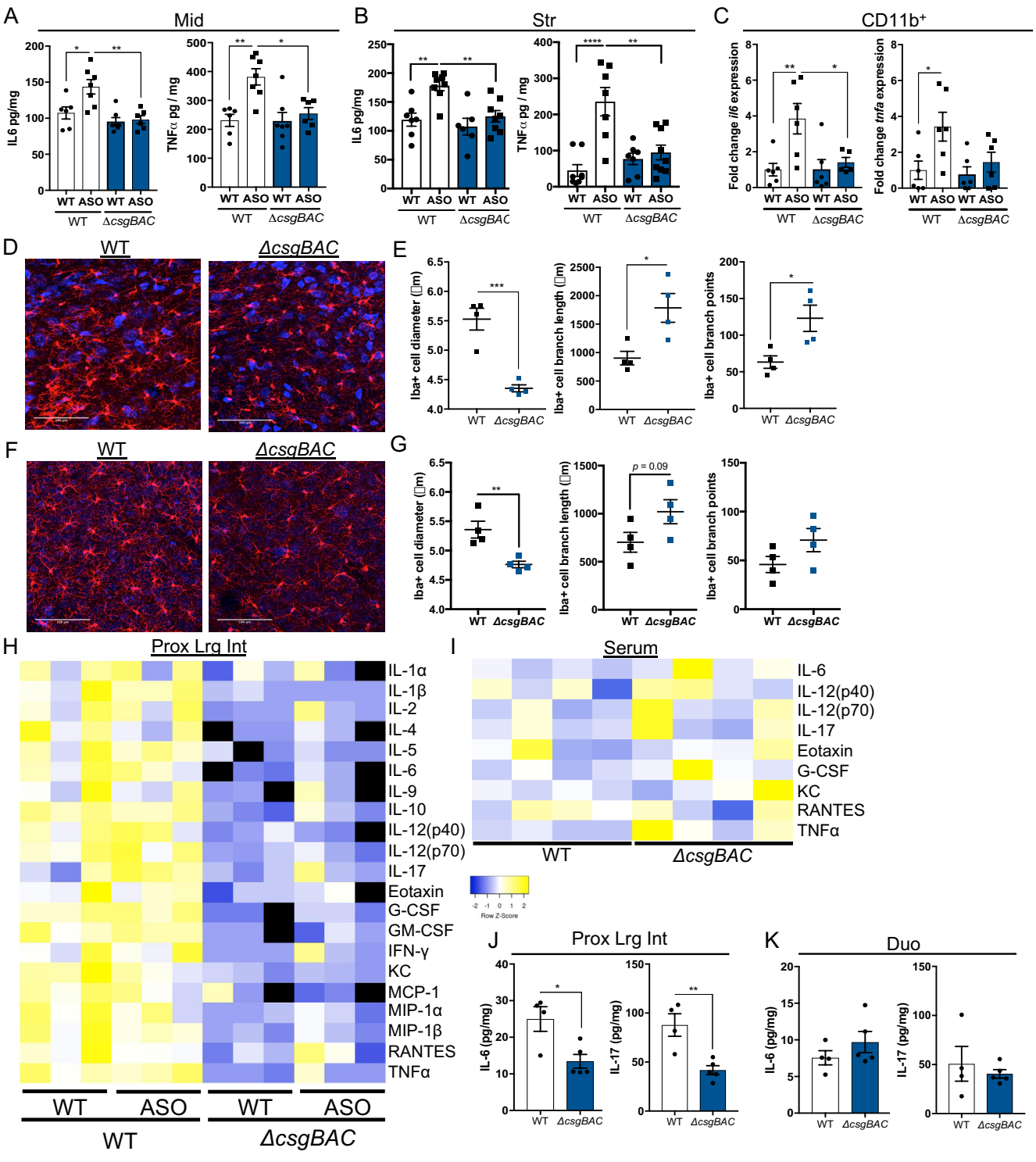

Figure 1—figure supplement 3. Mono-colonization with curli-sufficient bacteria induces altered inflammatory responses in the brain and intestine. Germ-free (GF) wild-type (WT) or Thy1-αSyn (ASO) animals were mono-colonized with either wild-type, curli-sufficient *E. coli* (WT) or curli-deficient *E. coli* (Δ*csgBAC*). Quantification of IL-6 and TNFα by ELISA from homogenates derived from the (**A**) midbrain or (**B**) striatum. (**C**) CD11b^{+} cells enriched from total brains and gene expression of *il6* and *tnfa* quantified by qRT-PCR, relative to *gapdh*. Representative thin sections of (**D**) substantia nigra and (**F**) striatum derived from ASO mice stained for Iba1 (microglia). 3D cellular reconstructions of microglia generated and morphological characteristics

Figure 1—figure supplement 3 continued on next page

Figure 1—figure supplement 3 continued

quantified of (**E**) substantia nigra- and (**G**) striatum—resident microglia. Multiplex ELISA performed for cytokines and chemokines derived from (**H**) homogenates derived from proximal large intestine tissue of indicated animals or (**I**) serum of ASO animals. Quantification of IL-6 and IL-17 by ELISA from tissue homogenates of the (**J**) proximal large intestine or (**K**) duodenum derived from ASO animals. n = 6–7 (**A–C**), n = 4 (**D–G**) (averaged from 20 to 40 cells for diameters, or 5–7 cells for branching), n = 3 (**H**), n = 4–5 (**J, K**). Points represent individuals, bars represent the mean and standard error. Data analyzed by one-way ANOVA with Tukey post-hoc test for **A–C**), or two-tailed *t*-test for **E, J**) and **K**). *p≤0.05; **p≤0.01; ***p≤0.001; ****p≤0.0001. Scale bars = 100 μm.

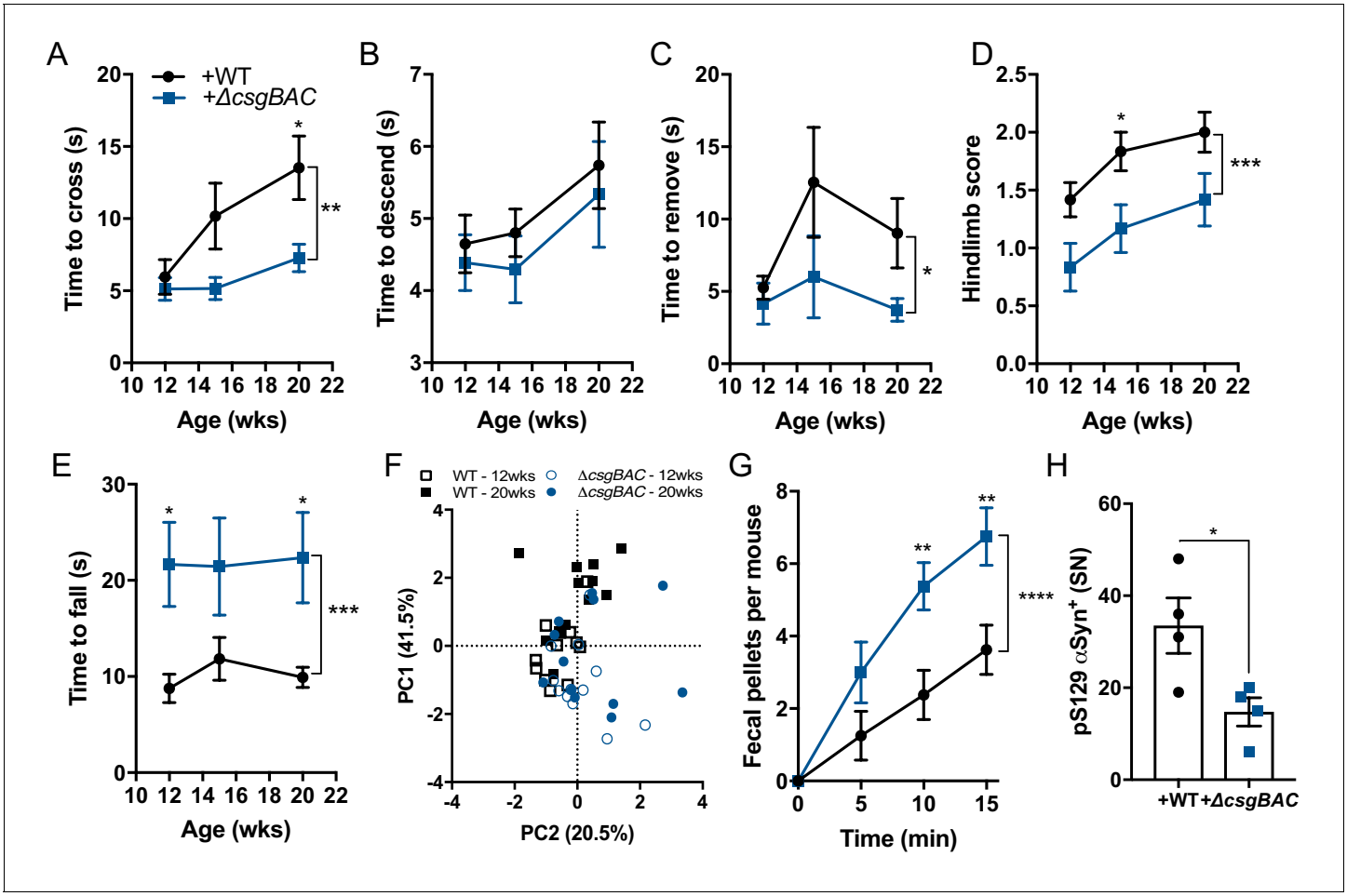

Figure 2. Curli biosynthesis within a complex microbiome contributes to motor and GI deficits Germ-free Thy1-αSyn (ASO) mice were colonized with fecal microbes derived from healthy human at 5–6 weeks of age, and concurrently supplemented with either wild-type *E. coli* MC4100 (+WT) or a curli-deficient strain (+Δ*csgBAC*). Motor function was tested longitudinally at 12, 15, and 20 weeks of age in the (**A**) beam traversal, (**B**) pole descent, (**C**) adhesive removal, (**D**) hindlimb clasping score, (**E**) wirehang tests. (**F**) Principal component analysis of compiled motor scores from tests in (**A–E**). (**G**) Fecal output over a 15-min period observed at week 21 of age. Quantification of (**H**) pS129αSyn by immunofluorescence microscopy in the substantia nigra. n = 12 (**A–F**), n = 6 (**G**), n = 4 (**H**). Data points represent individuals, bars represent the mean and standard error. Time courses analyzed by two-way ANOVA, with Sidak post-hoc test for between group comparisons indicated above individual time points, and brackets indicating significance between colonization status. Data in (**H**) analyzed two-tailed *t*-test. *p≤0.05; **p≤0.01; ***p≤0.001; ****p≤0.0001. Motor data are compiled from two independent cohorts.

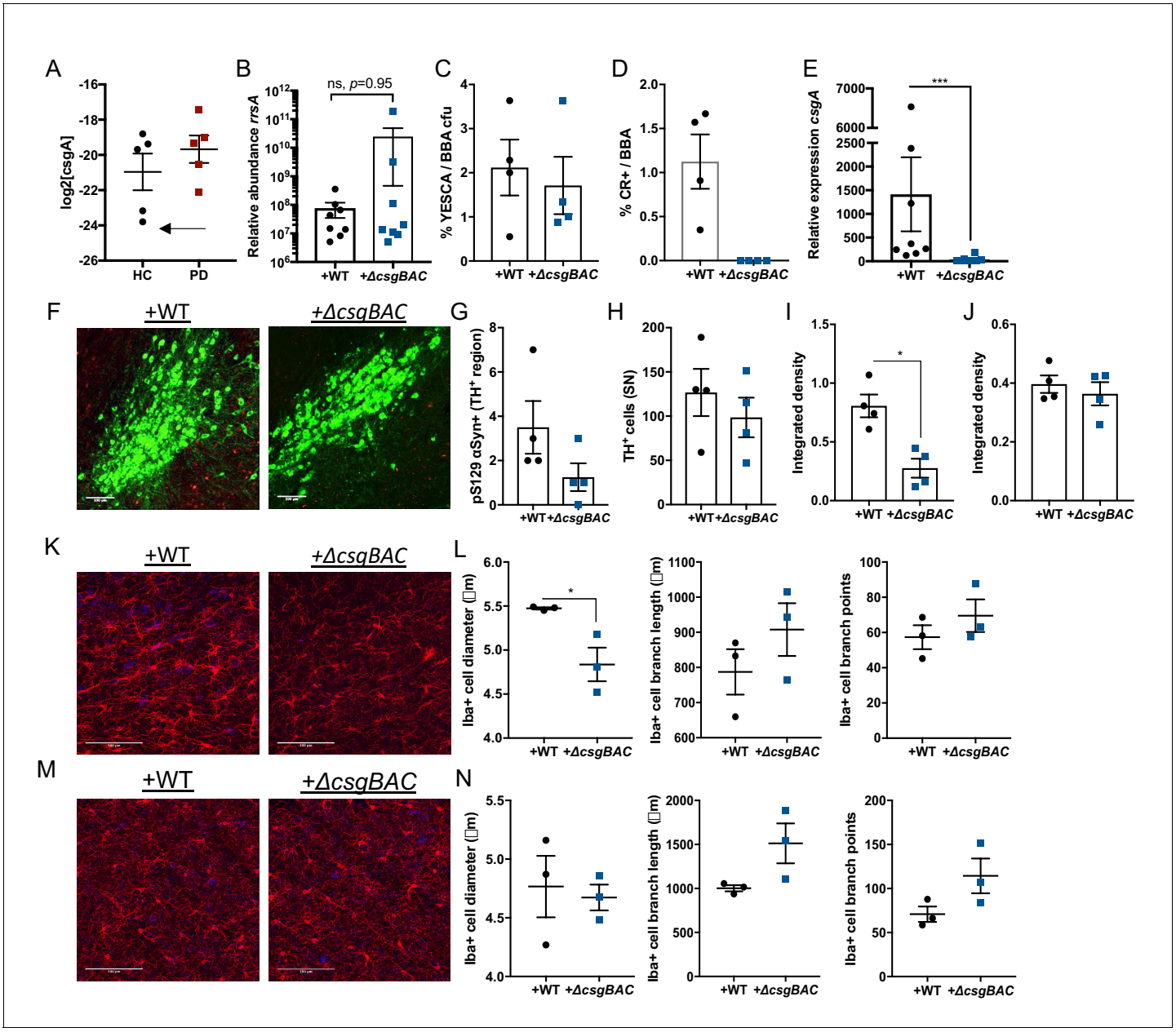

Figure 2—figure supplement 1. Amyloid-producing bacteria in humanized animals modulate microglia responses. (**A**) Human samples from previous cohort (ENA Accession: PRJEB17694) were analyzed by PICRUSt to infer abundance of *csgA* encoded within each population, arrow indicates sample utilized for transplantation. Fecal pellets of Thy1-αSyn (ASO) mice receiving healthy-human derived fecal microbes enriched with either wild-type, curli-sufficient *E. coli* (WT) or curli-deficient *E. coli* (Δ*csgBAC*) were analyzed by (**B**) qPCR for *rrsA* abundance relative to 16 s rRNA present in fecal bacterial DNA and ratios of (**C**) YESCA/blood agar aerobic colony forming units and (**D**) congo red-positive/blood agar colony forming units calculated. (**E**) qPCR analysis for *csgA* expression relative to *rrsA* in fecal bacterial RNA. (**F**) Representative images of the substantia nigra in humanized ASO mice stained for TH (green) and pS129 (red) and quantified in (**G, H**). Quantification of insoluble αSyn fibrils in the (**I**) midbrain and (**J**) striatum by dot blot assay. Representative thin sections of (**K**) substantia nigra and (**M**) striatum derived from ASO mice stained for Iba1 (microglia; red). 3D cellular reconstructions of microglia generated and morphological characteristics quantified of (**L**) substantia nigra- and (**N**) striatum—resident microglia. n = 5 (**A**), n = 8 (**B, E**), n = 4 (**C–J**), n = 3 (**K–N**) (averaged from 20 to 40 cells for diameters, or 5–7 cells for branching) Points represent individuals, bars represent the mean and standard error. Data in (**B, E, I**) analyzed by two-tailed Mann-Whitney test or t-test in **L**. *p≤0.05; ***p≤0.001. Scale bars = 100 μm.

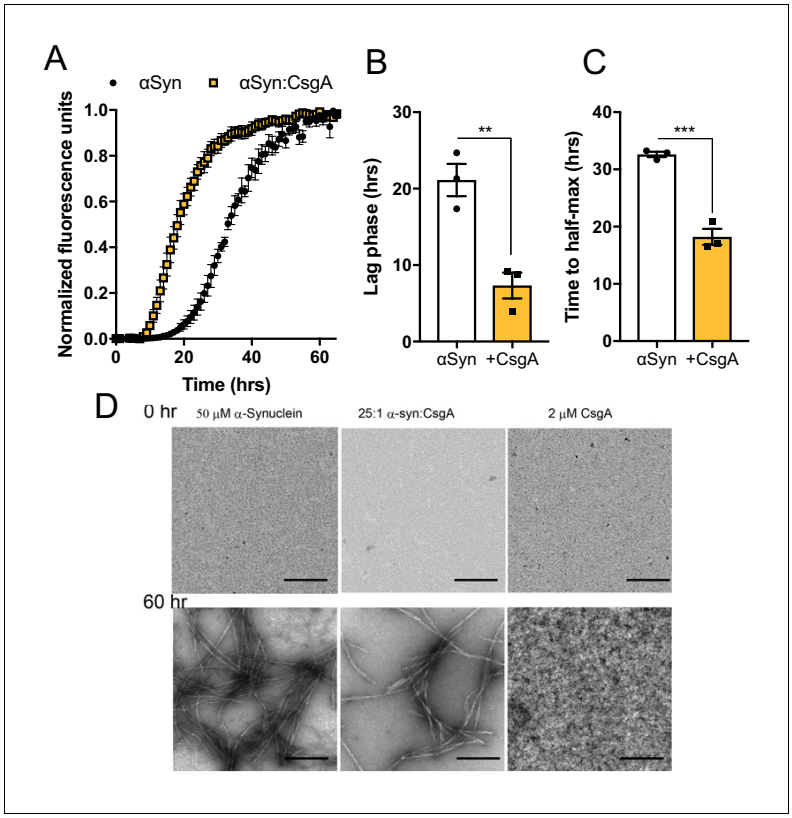

Figure 3. The bacterial amyloid protein, CsgA, accelerates αSyn fibrilization In vitro biophysical analysis with purified αSyn and CsgA proteins. (**A**) Aggregation as measured by Thioflavin T fluorescence over time during αSyn amyloid formation alone or in the presence of CsgA monomers (25:1 molar ratio). Time to reach (**B**) exponential fibrilization/lag phase and (**C**) half-maximum from reactions in (**A**). (**D**) Representative transmission electron micrographs of αSyn or CsgA alone, or in combination, at 0 and 60 hr post-aggregation. n = 3 (**A–C**). Bars represent the mean and standard error. Data are analyzed by two-tailed, *t*-test. **p≤0.01; ***p≤0.001.

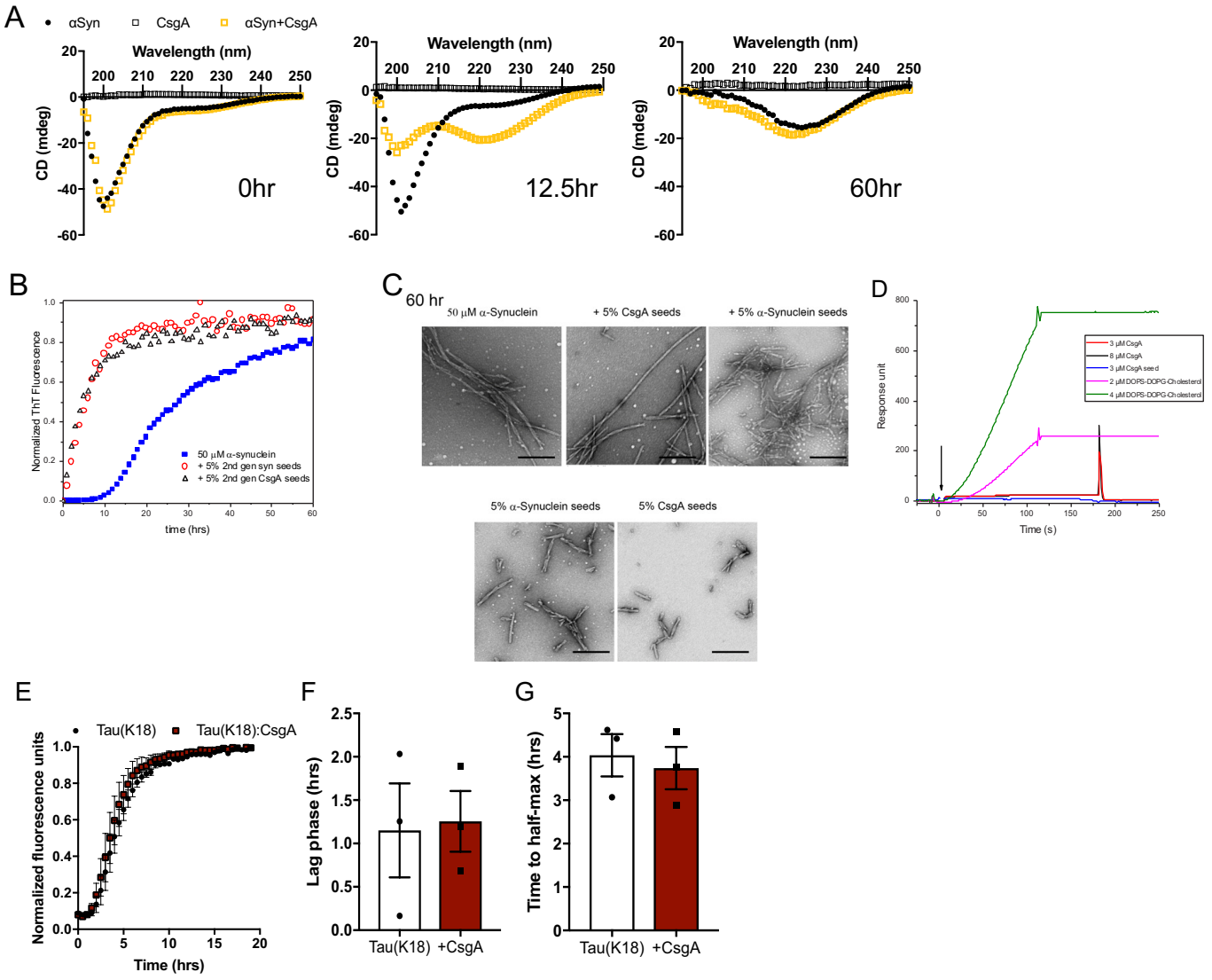

Figure 3—figure supplement 1. CsgA seeds αSyn aggregation and propagation in vitro. (**A**) Circular dichroism spectroscopic analysis of αSyn fibrilization alone or in the presence of CsgA at 0, 12.5, and 60 hr post-aggregation. (**B**) Thioflavin T fluorescence during αSyn amyloid formation alone or in the presence of 5% seeds previously generated by addition of CsgA monomer to αSyn (as in ***Figure 2a***) or αSyn alone. (**C**) Transmission electron micrograph of fibril structures generated by the addition of above seeds and of seeds themselves. (**D**) Surface plasmon resonance measurements of surface immobilized αSyn with additions of either CsgA monomer or seeds, or DOPS-DOPG cholesterol liposomes as positive control. (**E**) Amyloid aggregation as measured by Thioflavin T fluorescence with Tau alone or in the presence of CsgA monomers (25:1 molar ratio, red). Time to reach (**F**) exponential fibrilization/lag phase and (**G**) half-maximum from reactions in (**E**).

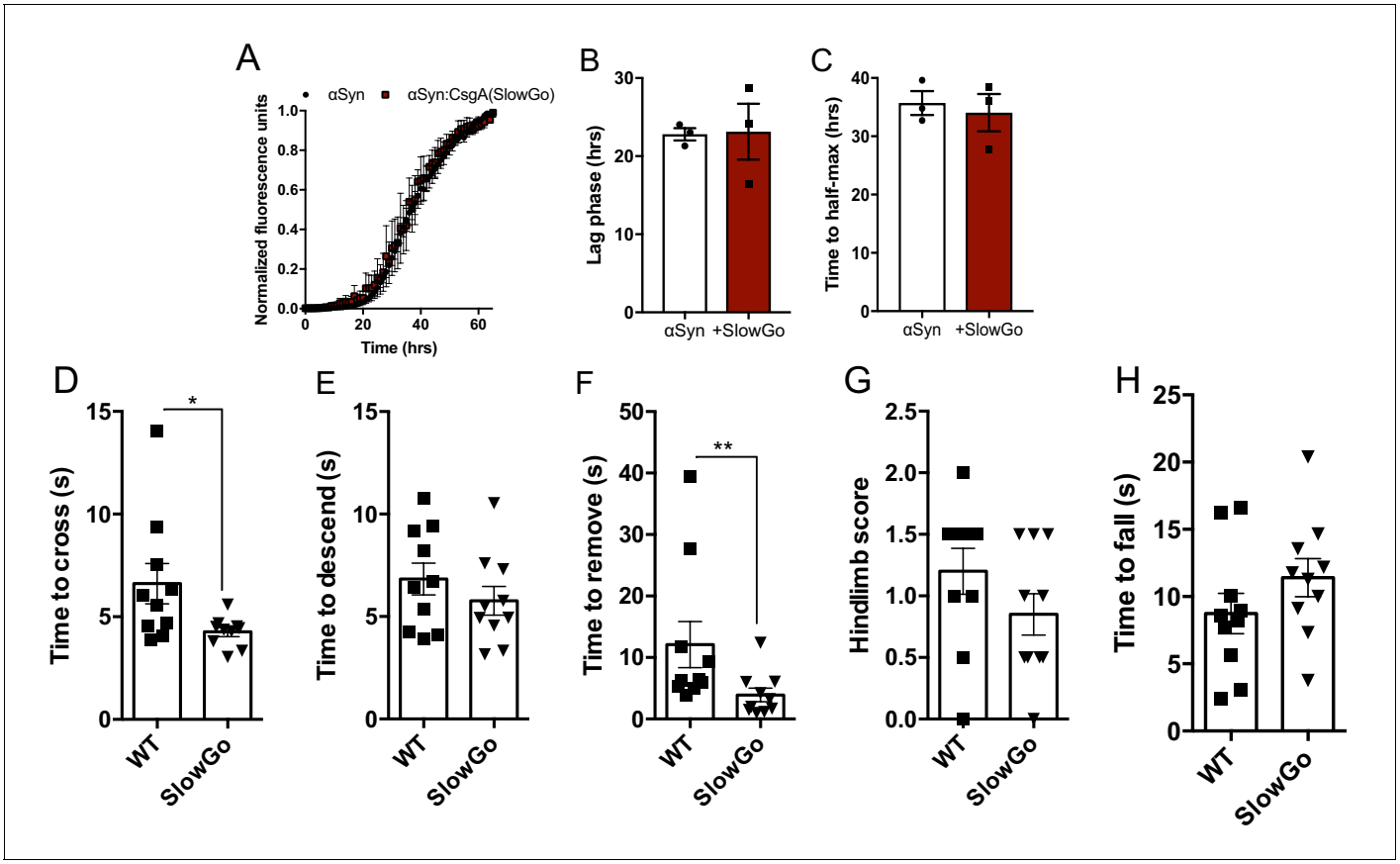

Figure 3—figure supplement 2. CsgA seeds αSyn aggregation in vitro and in vivo through native amyloidogenic properties. (**A**) Amyloid aggregation as measured by Thioflavin T fluorescence with αSyn alone or in the presence of non-amyloidogenic CsgA monomers (SlowGo, 25:1 molar ratio, red). Time to reach (**B**) exponential fibrilization/lag phase and (**C**) half-maximum from reactions in (**A**). (**D–H**) Germ-free Thy1-αSyn mice (ASO) were mono-colonized with *E. coli* producing either wild-type CsgA (WT) or SlowGo (SlowGo), and motor function assessed at 12-13 weeks of age in (**D**) beam traversal, (**E**) pole descent, (**F**) adhesive removal, (**G**) hindlimb reflexes, and (**H**) wirehang. Points represent individuals, bars represent the mean and standard error, n = 10–11 (**D–H**). Data in (**D–H**) analyzed by two-tailed Mann-Whitney test. *$p \leq 0.05$; **$p \leq 0.01$.

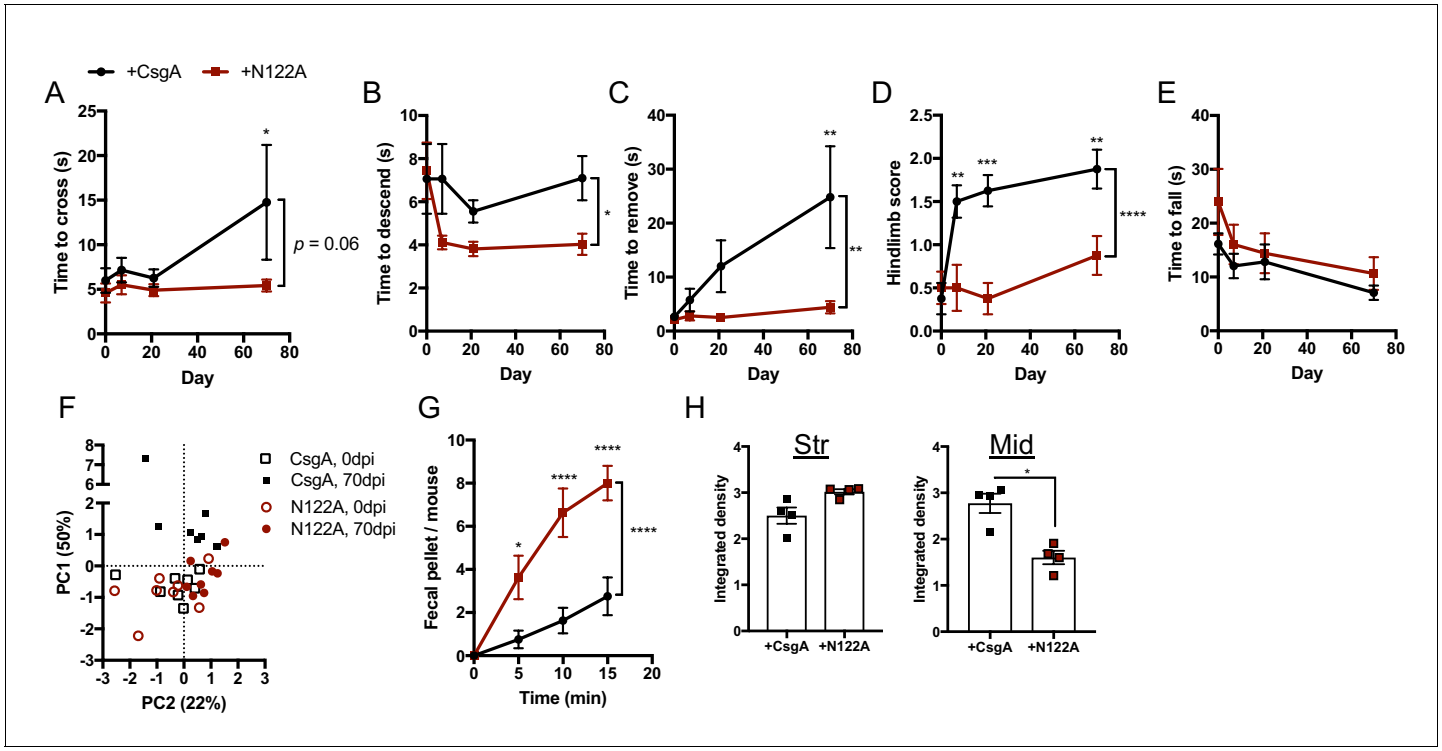

Figure 3—figure supplement 3. Intestinal injection of amyloidogenic curli promotes progressive motor dysfunction. Conventionally-raised Thy1-αSyn (ASO) mice were injected intestinally with 30 μg of synthetic CsgA hexamer (CsgA; N-QYGGNN-C) or non-amyloidgenic peptide (N122A; N-QYGGNA-C). Motor function assessed overtime at 0, 7, 21, and 70 days post-injection in the (**A**) beam traversal, (**B**) pole descent, (**C**) adhesive removal, (**D**) hindlimb clasping score, and (**E**) wirehang tests. (**F**) Principal component analysis of compiled motor scores of ASO mice. (**G**) Fecal output observed at day 70 in ASO mice. (**H**) Quantification of insoluble αSyn fibrils in the striatum and ventral midbrain by dot blot assay. n = 8 (**A–G**), n = 4 (**H**). Points represent individuals, bars represent the mean and standard error. Time courses analyzed by two-way ANOVA, with Sidak post-hoc test for between group comparisons indicated above individual time points, and brackets indicating significance between treatments. Data in (**H**) analyzed by two-tailed Mann-Whitney test. *p≤0.05; **p≤0.01; ***p≤0.001; ****p≤0.0001.

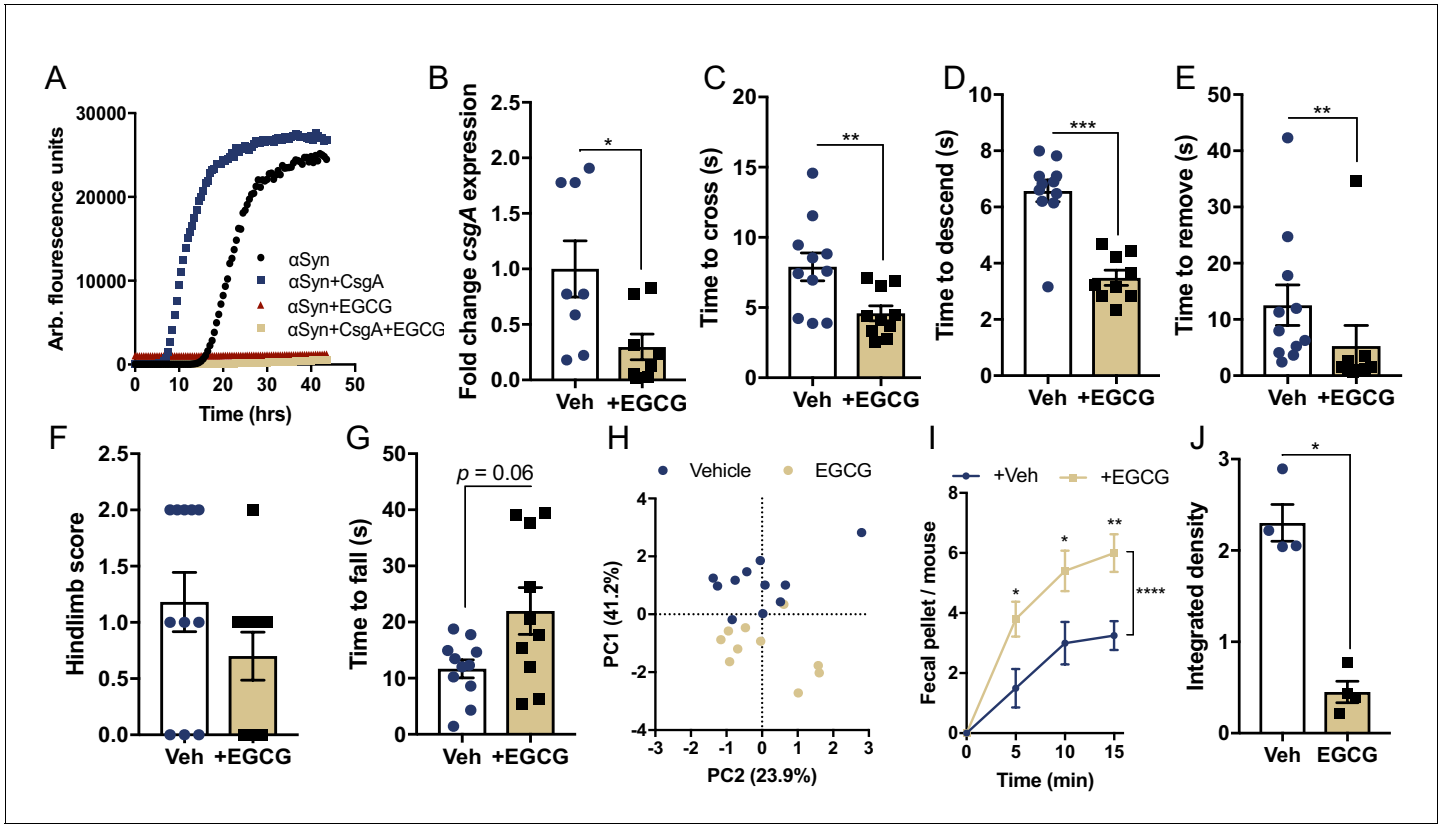

Figure 4. Curli-driven pathophysiology in mice requires functional amyloid formation. (**A**), Representative in vitro αSyn aggregation measured by Thioflavin T fluorescence during αSyn amyloid formation alone or in the presence of CsgA (25:1 molar ratio), with and without EGCG (50 μM) treatment. (**B–H**) Germ-free Thy1-αSyn mice (ASO) were mono-colonized with WT *E. coli* at 5–6 weeks of age, and given water alone (Vehicle: Veh) or treated with EGCG *ad lib* in drinking water (+EGCG). (**B**) RNA was extracted from fecal pellets and *csgA* expression quantified by qRT-PCR, relative to *rrsA*. Motor function was assessed at 15–16 weeks of age by quantifying (**C**) beam traversal time, (**D**) pole descent time, (**E**) nasal adhesive removal time, (**F**) hindlimb clasping score, (**G**) wirehang tests. (**H**) Principal component analysis of compiled motor scores from tests in (**C–G**). (**I**) Fecal output over a 15 min period. (**J**) Quantification of insoluble αSyn fibrils in the ventral midbrain by dot blot assay. n = 8 (**B**); n = 10–11 (**C–G**); n = 4–5 (**I, J**). Points represent individuals, bars represent the mean and standard error. Data analyzed by two-tailed Mann-Whitney for **B–G**, (**J**) and two-way ANOVA with Sidek's post-hoc test for **I** with between group comparisons indicated above individual time points, and brackets indicating significance between treatment status. *p≤0.05; **p≤0.01; ***p≤0.001; ****p≤0.0001. Motor data compiled from two independent cohorts.

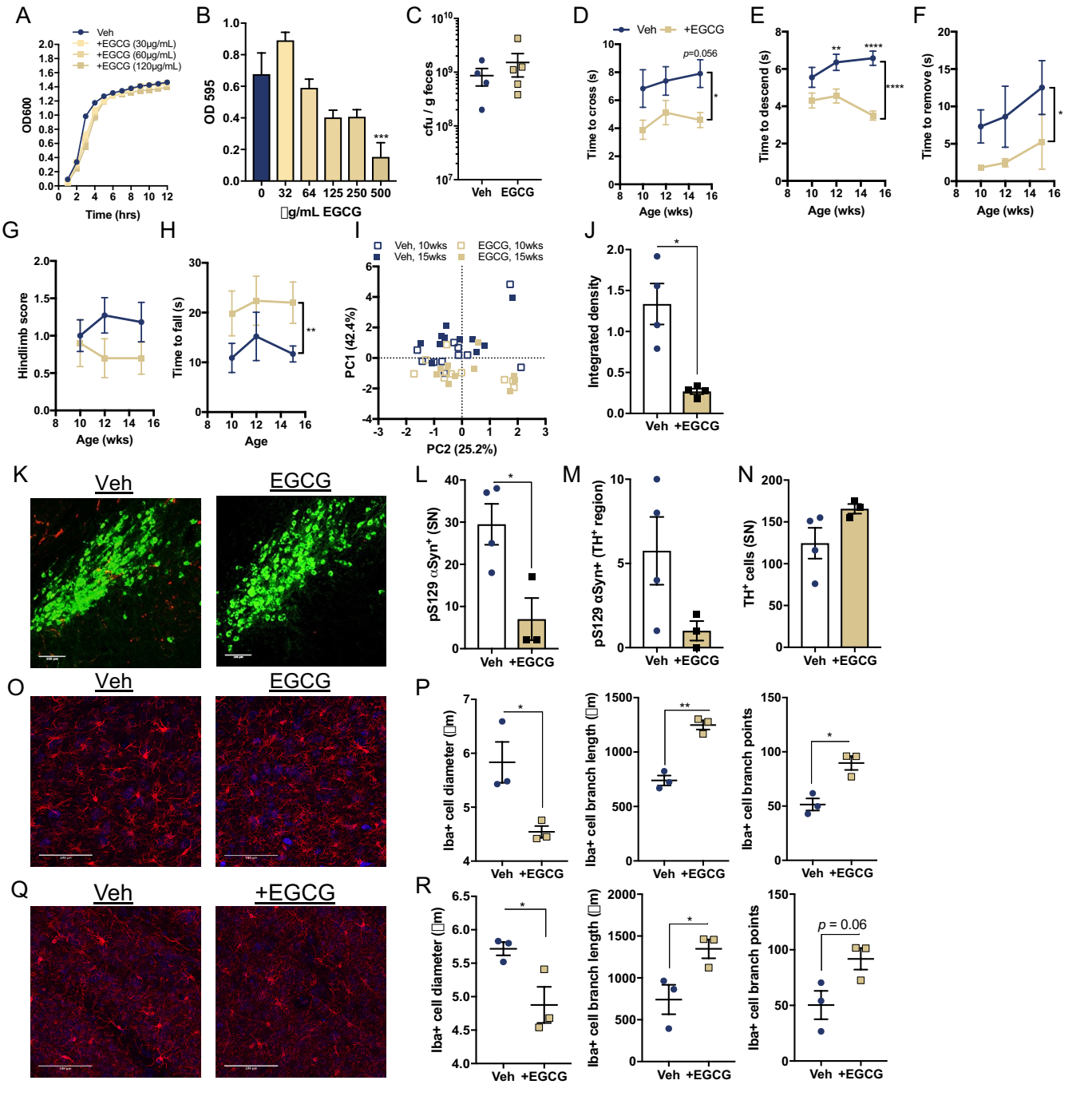

Figure 4—figure supplement 1. Inhibition of functional amyloid formation dampens progressive pathophysiology. (**A**) Wild-type *E. coli* was inoculated into brain-heart infusion broth, containing indicated concentrations of EGCG. Cultures were incubated, with orbital shaking and growth was measured by optical density at 600 nm over time. (**B**) Crystal violet staining of wild-type *E. coli* biofilm at 4 days in static culture, with indicated concentrations of epigallocatechin gallate (EGCG); assessed by optical density (OD). (**C–R**) Germ-free ASO mice were mono-colonized with wild-type *E. coli* and treated with water alone (Vehicle, Veh) or given EGCG *ad lib* in drinking water (+EGCG). (**C**) Fecal pellets were cultured on YESCA agar to determine total viable *E. coli*. Motor function was assessed at 10, 12, and 15 weeks of age by quantifying (**D**) beam traversal time, (**E**) pole descent time, (**F**) nasal adhesive removal time, (**G**) hindlimb reflex score, (**H**) wirehang tests. (**I**) Principal component analysis of compiled motor scores. (**J**) Quantification of insoluble αSyn fibrils in the striatum by dot blot assay. (**K**) Representative images of the substantia nigra in humanized ASO mice stained for TH (green) and pS129 (red) and quantified in (**L–N**). Representative thin sections of (**O**) substantia nigra and (**Q**) striatum were stained for Iba1 (microglia; red) and

Figure 4—figure supplement 1 continued on next page

Figure 4—figure supplement 1 continued

morphological characteristics of (**P**) substantia nigra- and (**r**) striatum-resident microglia quantified. n = 3 (**A, O–R**) (averaged from 20 to 40 cells for diameters, or 5–7 cells for branching); n = 6–7 (**B**); n = 4–5 (**C, J**), n = 10–11 (**D–I**); n = 3–4 (**K–N**). Points represent individuals, bars represent the mean and standard error. Time courses analyzed by two-way ANOVA, with Sidak post-hoc test for between group comparisons indicated above individual time points, and brackets indicating significance between treatments. Data in (**J**) analyzed by two-tailed Mann-Whitney test and (**L, P, R**) analyzed by two-tailed *t*-test. *$p \leq 0.05$; **$p \leq 0.01$; ****$p \leq 0.0001$.